# PARTICLES AT QUASI-PERPENDICULAR COLLISIONLESS SHOCKS: DEPENDENCE ON THE SHOCK SCALE

Michael Gedalin
Department of Physics
Ben-Gurion University, Beer-Sheva 84105, Israel

## ABSTRACT

We review the ion and electron heating at the quasi-perpendicular collisionless shock front. The shock width is between the typical ion length (ion drift gyroradius) and electron scale (electron inertial length) which results in the different behavior of these two species. Ions are effectively heated at the ramp and/or reflected due to the strong breakdown of adiabaticity and direct conversion of the directed flow energy into the ion gyration energy. Electrons are dragged across the shock by the electric field along the magnetic field, if the shock is not very narrow. At even smaller shock widths electrons become nonadiabatic also and the acceleration occurs along the shock normal. Because of the direct relation of the heating features to the shock scales, the former may serve a tool for additional indirect determination of the scales.

## I. INTRODUCTION

Collisionless shock is a good example of a system which is intrinsically multiscale. A naive MHD point of view, which is applicable for the very large scale average picture of the shock, resolves a discontinuity, on which the magnetic field, density, and pressure jumps, and the bulk plasma velocity drop occur. When viewing the shock with a magnifying glass, one first resolves (simply large scales) extended regions of turbulence accompanying the discontinuity. At medium and fine scales the quasi-perpendicular collisionless shock possesses a well-defined quasi-stationary and quasi-one-dimensional structure, while at even smaller scales highly time–dependent wavy shape would be observed. All these scales are intrinsically inter-related, and the shock features at a definite scale depend on its features at other scales. In the present paper we discuss the medium and fine scales. To the medium scale we attribute the shock foot, which is a rather extended ($\sim V_u/\Omega_i$) part of the shock front, on which the magnetic field and density increase, and the plasma bulk velocity decreases gradually. The fine scale is represented by the ramp, which is the most narrow (between $c/\omega_{pi}$ and $c/\omega_{pe}$) part of the shock stationary structure, and on which the main magnetic jump occurs. We consider the processes which lead to ion and electron heating in these regions and discuss the interrelation of these two scales and the particular importance of the fine scale for the whole shock life.

## II. ION REFLECTION

A foot forms when some ions are reflected off the shock transition layer (that is, ramp). In a simplest model [1] a perpendicular shock is assumed to be a discontinuity at $x = 0$ (the shock normal is along $x$, and the magnetic field is $\mathbf{B} = (0, 0, B)$), and ions are reflected specularly, that is, the normal component changes its sign $v_x \rightarrow -v_x$, while the tangential component does not change $v_y \rightarrow v_y$.

The ion velocity deviation from the bulk plasma velocity $u_x, u_y \sim v_T = V_u(\beta_i/2M^2)^{1/2}$, where $\beta_i = 8\pi n_i T_i/B^2$, and $M = V_u/v_A$ is the upstream Mach number. For a supercritical shock at 1 AU typical $\beta_i \sim 1$ and $M \approx 5$, so $v_T/V_u \leq 0.15$. For our present goals it would suffice to make an approximation $v_T/V_u \ll 1$. In this case the reflected ions turn back toward the shock almost in the same point $X \approx 0.68\, V_u/\Omega_i \pm O(v_T/V_u)$. The ions form a semi-ring in the configuration space with the velocity spread $|v_x| \lesssim (v_T V_u)^{1/2}$, $|v_y - V_u\sqrt{3}| \lesssim (v_T V_u)^{1/2}$ near the turning point. The corresponding $y$ component of the ion current $j_y \sim n_T e V_u \sqrt{3} \sim (c/4\pi)(dB_z/dx)$ (where $n_T$ is the ion density near the turning point) is responsible for the gradual increase of the magnetic field, which is observed as a magnetic foot. The turning distance $X_0 = 0.68\, V_u/\Omega_i$ is in this case the (approximate) foot length.

The above consideration was generalized onto ion specular reflection in the oblique case to derive approximate expression for the foot length in [2] and improved in [3] to give the following expression

$$\Omega_i d/V_u = f(\theta) = \Omega_i t_0(2\cos^2\theta - 1) + 2\sin^2\theta\, \sin(\Omega_i t_o), \tag{1}$$

$$\cos(\Omega_i t_0) = (1 - 2\cos^2\theta)/2\sin^2\theta. \tag{2}$$

This expression agrees with the observational data within $50\%$ error [3]. The discrepancy can be attributed to the difficulties of the foot determination in supercritical shocks, because of the finite ramp width and magnetic field oscillations persisting well into upstream region. Another source of the error is the nonspecular character of the ion reflection. It should be mentioned that the above expressions do not distinguish between supercritical and subcritical shocks, while observations show that there is no foot at all in subcritical $M < M_c$ shocks.

The ion ring should be directly observed as a gyrophase bunched distribution in the ion velocity space.Indeed, observations [4] show presence of a strong gyrophase bunched component of the ion distribution in supercritical shocks, where they appear first when the observer enters the foot and persist well into downstream region, experiencing gradual deformation (upstream) and smearing out (downstream). Weaker gyrophase bunched components are observed in subcritical shocks just behind the ramp (or in the ramp itself), which are also smeared out while progressing more downstream.

## III. ION HEATING

Since the reflected and transmitted to the downstream region (at their second encounter with the ramp) ions constitute a rather energetic gyrophase bunched component of the ion distribution, these ions contribute significantly to the ion heating. It was proposed that the reflected ions are responsible for the strong overadiabatic ion heating at the quasi-perpendicular shock front. This mechanism works for supercritical shocks, where the reflected ion fraction can be large ($>$ $5\%$), but it is irrelevant for subcritical shocks where the reflected ion fraction is negligible ($< 1\%$).

Another mechanism was proposed in [5] based on the difference between adiabatic and nonadiabatic ion trajectories in the ramp. It was assumed that nonadiabatic ions have not enough time to be substantially deflected from their initial direction of motion in the ramp.

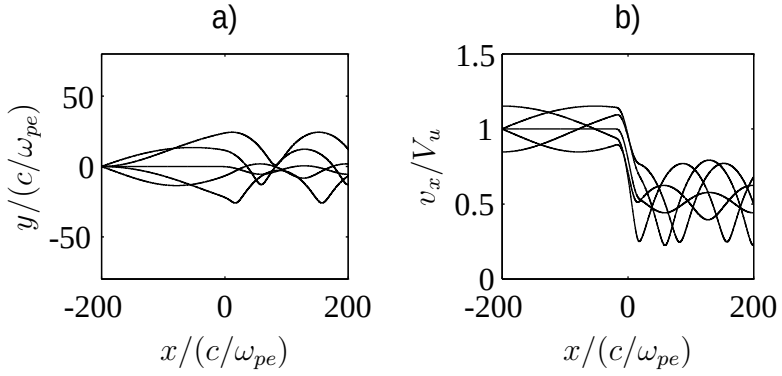


Figure 1: Ion trajectories in the subcritical case

Hence, an ion coming from the upstream region along the upstream magnetic field will proceed, after crossing the ramp, along the same upstream magnetic field, that is, at a substantial angle to the local (downstream) magnetic field. The immediate gyration velocity is $\approx V_u \sin\theta_{ud}$, where $V_u$ is the upstream plasma velocity, and $\theta_{ud}$ is the angle between the upstream and downstream magnetic fields.

The resulting heating has been illustrated by numerical simulations [6] (one-dimensional hybrid code). It was shown that the ion distribution in supercritical shocks contains strong gyrophase bunched components which are responsible for the strong ion heating. In the subcritical regime there are almost no reflected ions and the downstream distribution is simply much more wide in the velocity space, than the upstream distribution (although apparently non-Maxwellian).

This approach was criticized [7], especially the assumption of the absence of deflection. In the more comprehensive numerical simulations (one-dimensional

hybrid code) the relative importance of the directly transmitted and reflected ions was studied. It was shown that all ion heating is due to the directly transmitted ions in the subcritical case and the heating front is positioned at the ramp. The role of the reflected ions becomes progressively more important with the increase of the supercriticality $M/M_c$, and they quickly begin to dominate in the ion heating. The heating front moves well into the upstream region. Kinetic effects were claimed to be important in the ion heating process.

Despite the criticism of [7], actually both [6] and [7] describe the same physical effect, namely, the nonadiabaticity of the ion motion in the ramp and dependence of this nonadiabaticity on the ramp width. This dependence is shown in Figs. 1 and 2, where several ion trajectories in two cases (subcritical and supercritical) are presented. In each case five ions, one without initial gyration velocity and other four with the gyration velocity of $v_T$ and different initial phases ($0^\circ$, $90^\circ$, $180^\circ$, and $270^\circ$) enter the ramp.

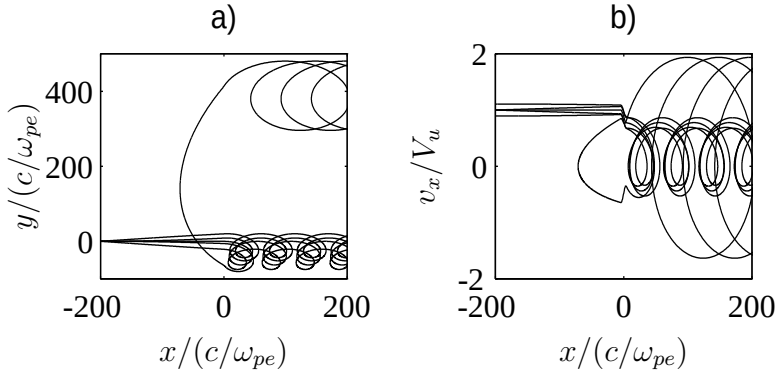


Figure 2: Ion trajectories in the supercritical case

The subcritical regime shown in Fig. 1 is characterized by the following parameters: $M = 2$, $B_{zd}/B_{zu} = 2$, and $\beta_i = 0.2$. In the supercritical regime (Fig. 2) $M = 7$, $B_{zd}/B_{zu} = 6$, and $\beta_i = 1.2$. In both cases the angle between the shock normal and the upstream magnetic field is $\theta = 75^\circ$. The ramp width is chosen to be equal $L_W = 2\pi c \cos\theta/\omega_{pi}(M^2-1)^{1/2}$, which is $\approx c/\omega_{pi}$ for the subcritical regime and $\approx 0.2c/\omega_{pi}$ in the supercritical case. The HTF cross-shock potential was chosen as $0.2m_iV_u^2/2$. The model shock structure used in this analysis was described in [8, 9].

One can see that there are no reflected ions in the subcritical case. The downstream velocity space occupied by the ions is clearly wider than the initial occupied velocity space. In the supercritical case only a fraction of the ion distribution (one ion in our case) is reflected, acquiring a large gyration energy and contributing significantly into the downstream temperature. The reflection is

clearly nonspecular and the turning distance is clearly smaller than the classical $0.68V_u/\Omega_i \approx 200(c/\omega_{pe})$ in the present case.

## IV. RAMP WIDTH

It is not known what determines the ramp width. Observations of the magnetic ramp width in subcritical shocks have been compared [10] to different theoretically predicted lengths, corresponding to several models, including the weak ion sound turbulence model and marginal stability hypothesis. It was found that all theoretical lengths are $\sim c/\omega_{pi}$, and there is a more or less satisfactory agreement (within 100% error) between the predictions and the measured ramp width. Later it was found [11, 12] that the ramp width is of the order of the phase-standing whistler precursor wavelength $L_W = 2\pi c \cos\theta/\omega_{pi}(M^2-1)^{1/2}$, even if this precursor is absent. For subcritical shocks this length is also of the order $c/\omega_{pi}$.

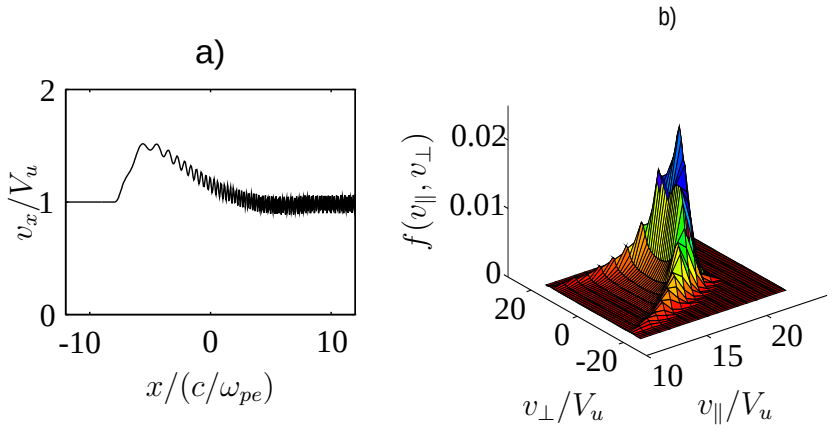


Figure 3: The initially nongyrating electron trajectory (a) and the downstream electron distribution (b) in the adiabatic case.

The ramp features in supercritical shocks are studied much worse. There is no statistical analysis of the ramp widths. In the only well documented supercritical shock [13] with $M = 7.7$ it was found that the ramp width is $\approx L_W \approx 8(c/\omega_{pe})$. Recently [14] it was shown that the ramp of a supercritical shock can be as narrow as $2(c/\omega_{pe})$, and the ramp itself can consist of several sub-jumps.

The electric field in the ramp is known even worse. Low-resolution measurements show [15] that the overall NIF cross-shock potential drop $\Delta\varphi \sim m_i V_u^2/2$. The ramp itself is not resolved in these measurements and the information about scales is lost. High-resolution electric field measurements are very rare and mainly on subcritical shocks. These measurements [16] show that the most of the cross-shock potential drop is applied at the ramp, and there is a pronounced electric field peak just inside the ramp. The scales of these electric field can be as

small as $c/\omega_{pe}$.

## V. ELECTRON HEATING

It is widely believed [17] that the electron heating at quasi-perpendicular shocks is due to the cross-shock potential. The mechanism of the heating depends strongly on the spatial scale of the variation of the cross-shock potential. In the adiabatic scenario [18] the electric field gradient is small $\alpha = -e(dE_x/dx)/m_e\Omega_e^2 \ll 1$ and the electrons are effectively accelerated along the magnetic field by the parallel component of the electric field. Most of the HTF cross-shock potential (which is the net energy budget for electrons) is transferred into the longitudinal degree of freedom. The electron perpendicular energy varies adiabatically $v_\perp^2 \propto B$ due to magnetic compression. The corresponding electron trajectory is shown in Figure 3a for the model shock parameters $M = 7$, $R = 6$, $e\varphi^{HTF} = 0.25 m_i V_u^2/2$, and the ramp width of $16(c/\omega_{pe}) \approx 0.4(c/\omega_{pi})$. The electron enters the ramp with a negligible gyration velocity. The downstream gyration remains negligible. The distribution $f(v_\parallel, v_\perp) = \int f(v_\parallel, v_{\perp 1}, v_{\perp 2}) dv_{\perp 2}$, which is formed at this step from an initial Maxwellian distribution with $v_T/V_u = 2.5$ is shown in Figure 3b. The downstream distribution is a strongly accelerated electron beam, which is weakly (adiabatically $T_\perp \propto B$) heated in the perpendicular and cooled in the parallel direction. At the following stage the distribution should

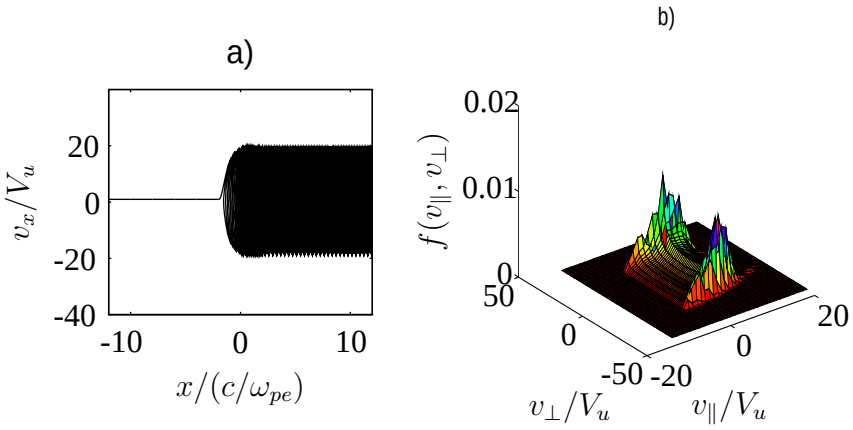


Figure 4: The initially nongyrating electron trajectory (a) and the downstream distribution of heated electrons (b) in in the nonadiabatic case.

be made nearly isotropic by filling the gap in the distribution either by some pre-existing electron population [18] or due to irreversible processes [19]. In the former case the downstream distribution and temperature are determined by the pre-existing electrons. In the latter case strong pitch-angle diffusion is required,

which in turn requires rather extended region of particle–turbulence interaction. Observations, however, show [18, 13] that electrons are heated promptly at the very upstream edge of the shock transition layer and the heating region is not resolved.

Nonadiabatic scenario was proposed recently [20, 8] for the shocks where the electric field gradients are large $\alpha \gtrsim 1$. In this case an electron is efficiently accelerated across the magnetic field and along the shock normal. A large fraction of the HTF cross-shock potential is transferred directly into the electron perpendicular energy (see Fig. 4a with the same shock parameters and the ramp width of $4(c/\omega_{pe})$). Respectively, the downstream distribution which forms at the first step, is quite different from the adiabatic one (see Fig. 4b). The electron beam is strongly deccelerated relative to the adiabatic regime. The strong overadiabatic heating in the perpendicular direction $T_{\perp d}/T_{\perp u} = (B_d/B_u)$ is accompanied by the corresponding heating in the parallel direction. The sections of the distribution along $v_\perp = 0$ and $v_\parallel = 0$ are no longer Maxwellian but resemble flattop distributions observed for the shocks with strong heating [18]. At the following step no pitch-angle diffusion is required and the distribution relaxation to the quasi-isotropic shape can be much faster than in the adiabatic case.

## VI. CONCLUSIONS

The global shock features, such as ion and electron heating, depend strongly on the features of the ramp, which is the most narrow part of the shock stationary structure. The more narrow is the ramp the more violent are the processes which lead to the particle energization on the shock front. Ion reflection becomes stronger with the increase of supercriticality and decrease of the ramp width. Ion motion is always nonadiabatic in the shock front, but this nonadiabaticity becomes stronger when the ramp width decreases. In the narrow ramp of a supercritical shock the electron motion can also become nonadiabatic which results in a strongly enhanced perpendicular energization of electrons and their nonadiabatic heating.

To summarize, the most narrow part of the shock is responsible for the most energetic processes at the shock front. The consequences of these processes are observed at scales which are by many orders of magnitude greater than the scale of the ramp itself. On the other hand, the features of the ramp should be determined by the global shock parameters, such as Mach number, $\beta$, angle between the shock normal and magnetic field, *etc.*. Therefore, bootstrap can be expected. Determination of this bootstrap remains an unresolved problem of the shock physics.

## REFERENCES

[1] L.C. Woods, J. Plasma Phys. **13**, 289 (1971).

[2] W.A. Livesey, C.T. Russell, and C.F. Kennel, J. Geophys. Res. **89**, 6824 (1984).
[3] J.T. Gosling and M.F. Thomsen, J. Geophys. Res. **90**, 9893 (1985).
[4] N. Sckopke, G. Paschmann, S.J. Bame, J.T. Gosling, and C.T. Russell, J. Geophys. Res. **88**, 6121 (1983).
[5] L.C. Lee, C.S. Wu, and X.W. Hu, Geophys. Res. Lett. **13**, 209 (1986).
[6] L.C. Lee, M.E. Mandt, and C.S. Wu, J. Geophys. Res. **92**, 13438 (1987).
[7] W.P. Wilkinson, J. Geophys. Res. **96**, 17675 (1991).
[8] M. Gedalin, M. Balikhin, and V. Krasnosselskikh, Adv. Sp. Res. **15(8/9)**, 225 (1995).
[9] M. Gedalin, Eos Trans. AGU, **75(44)**, Fall Meet.Suppl., 549, 1994.
[10] C.T. Russell, M.M. Hoppe, W.A. Livesey, J.T. Gosling, and S.J. Bame, Geophys. Res. Lett. **9**, 1171 (1982).
[11] M.M. Mellott and E. W. Greenstadt, J. Geophys. Res. **89**, 2151 (1984).
[12] M.H. Farris, C.T. Russell, and M.F. Thomsen, J. Geophys. Res. **98**, 15285 (1993).
[13] J.D. Scudder, A. Mangeney, C. Lacombe, C.C. Harvey, T.L. Aggson, R.R. Anderson, J.T. Gosling, G. Paschmann, and C.T. Russell, J. Geophys. Res. **91**, 11019 (1986).
[14] J. Newbury and C.T. Russell, Geophys. Res. Lett., in press.
[15] J.D. Scudder, A. Mangeney, C. Lacombe, C.C. Harvey, and T.L. Aggson, J. Geophys. Res. **91**, 11053 (1986).
[16] J.R. Wygant, M. Bensadoun, and F.C. Mozer, J. Geophys. Res. **92**, 11109 (1987).
[17] C.C. Goodrich and J.D. Scudder, J. Geophys. Res. **89**, 6654 (1984).
[18] W.C. Feldman, in *Collisionless Shocks in the Heliosphere: Reviews of Current Research,* Geophys. Monogr. Ser., vol. 35, edited by R.G. Stone and B.T. Tsurutani, pp. 195-205, AGU, Washington, D.C., 1985.
[19] P. Veltri and G. Zimbardo, J. Geophys. Res. **98**, 13335 (1993).
[20] M. Balikhin, M. Gedalin, and A. Petrukovich, Phys. Rev. Lett. **70**, 1259 (1993).